Eur. Phys. J. D **2**, 15–20 (1998)

**THE EUROPEAN PHYSICAL JOURNAL D**



# Effect of the initial phase of the field in ionization by ultrashort laser pulses

E. Cormier[1,2,a] and P. Lambropoulos[3]

[1] Laboratoire des Collisions Atomiques, CPTMB[b], Université de Bordeaux I, 351 Cours de la Libération, 33405 Talence, France
[2] Service des Photons, Atomes et Molécules, DRECAM, Centre d'Études de Saclay, 91191 Gif-Sur-Yvette, France
[3] Max-Planck-Institut für Quantenoptik, Hans-Kopfermann-str. 1, 85748 Garching, Germany

Received: 4 November 1997/Revised: 21 January 1998/Accepted: 23 February 1998

**Abstract.** We report on observable new features related to ionization of atoms by laser pulses of only few cycles and some intensity. We show that for particular photo-electron energies, the angular distribution becomes asymmetric and that this asymmetry is related to the initial phase of the field.

**PACS.** 32.80.-t Photon interactions with atoms – 42.50.Dv Nonclassical field states; squeezed, antibunched, and sub-Poissonian states; operational definitions of the phase of the field; phase measurements – 32.80.Wr Other multiphoton processes

## 1 Introduction

Rapid technological developments during the last few years have led to the realization of ultrashort laser pulses (less than 10 fs) at optical frequencies and relatively high intensities reaching up to $10^{16}$ W/cm$^2$. This means that such pulses consist of a few optical cycles under some envelope defining the overall shape of the pulse (see Fig. 1). In addition, the repetition rate of these devices can be as high as 1 Ghz, a feature that allows for experiments with very low signal per pulse and will be important in our discussion later on. In a pulse of so few cycles, the events in every single cycle carry a significant weight in the overall process. And, since the initial phase of the field (as it is defined by $\phi$ in Eq. (4)) can be arbitrary, the presence of a partial cycle among a few complete cycles can be the source of unusual effects, which from the standard perspective of photo-interactions with long pulses of tens of cycles, may seem counter-intuitive. If we consider the time-dependent field as a sinusoid multiplied by a shaped envelope (Gaussian), changing the initial phase simply is equivalent to shift the sinusoid within the envelope on the time scale. Thus, since only very few cycles with different amplitudes are contained in the envelope, whether the field is pointing up, or down (which can be achieved by changing the initial phase) at the very time where the envelope is maximum, will dramatically alter the physical processes leading, for example, to ejection of electrons in either of the directions up or down. The obvious consequence of a short pulse, whose bandwidth can be assumed to be Fourier limited, is the broad spectral width. The more subtle consequences have to do with the sensitivity of a process like ionization to the details of the shape of the envelope and to the initial phase of the field to which it is intimately connected. The motivation for and the purpose of this work has been the exploration of the phenomena which are affected by these new features of such pulses and conversely to explore how well-studied aspects such as ionization may be exploited to detect, for example, the initial phase of the field or perhaps even its fluctuation from pulse to pulse.

[a] e-mail: eric@petrus.lcab.u-bordeaux.fr
cormier@spam.saclay.cea.fr
[b] UPRESA 5468

## 2 Theoretical description

The electron energy spectrum is obtained by solving the Time-Dependent Schrödinger Equation (TDSE) numerically. The method, in which the 3D wave function is expanded on a set of spherical harmonics and radial B-splines functions has been described elsewhere (see [1,2]). Since Alkali atoms have only one electron on the outermost energy shell, and considering the moderate field intensity used in our context, it is safe to assume that only the valence electron will play a role in the dynamics of the system. Therefore, the atom is modeled by a single active electron experiencing a pseudo-potential [3] accounting for the frozen inner electrons.

The approximations related to the interaction with the field are the ones commonly used in this type of computation, *i.e.* we work within the dipole approximation and the electromagnetic field is semi-classical with a Gaussian pulse shape. Atomic units are implied unless otherwise stated.

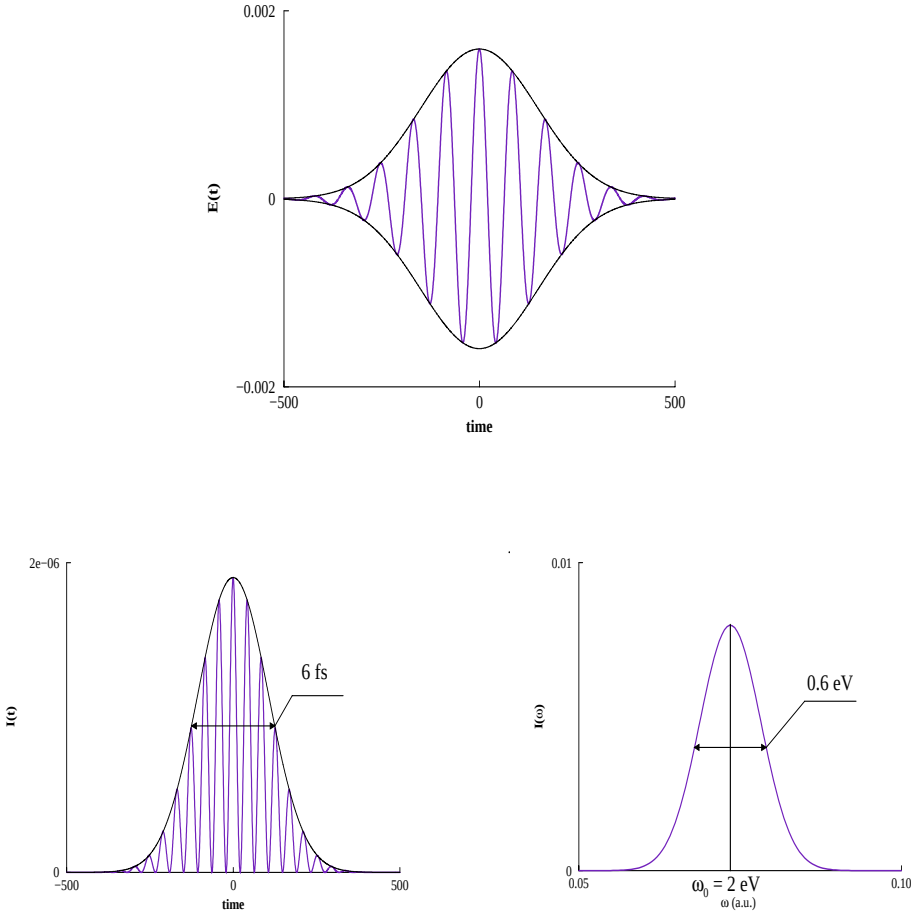


**Fig. 1.** Plot of the electromagnetic field used in this paper: the time-dependent field and intensity and the intensity in the frequency domain.

Once the TDSE is solved *i.e.* the state of the system is known at any time, the angular distribution of electrons ejected with energy $E_k$ is obtained at the end of the pulse *via* the following projection:

$$\frac{\partial P}{\partial E_k \partial \Omega_{\mathbf{k}}}(E_k, \theta_{\mathbf{k}}, \phi_{\mathbf{k}}) = |\langle f_{\mathbf{k}}^{(-)}(\mathbf{r}) | \psi(\mathbf{r}, t = T_{\text{final}}) \rangle|^2 \quad (1)$$

where $\psi(\mathbf{r}, t = T_{\text{final}})$ the total wave-function at the end of the pulse. The Coulomb wave $f_{\mathbf{k}}^{(-)}(\mathbf{r})$ is expanded in terms of spherical harmonics:

$$f_{\mathbf{k}}^{(-)}(\mathbf{r}) = \sum_{l=0}^{\infty} (i)^l \mathrm{e}^{-i\delta_l} \phi_{E_k}^l(\mathbf{r}) \mathrm{Y}_l^{0^*}(\theta_{\mathbf{k}}, \phi_{\mathbf{k}}) \quad (2)$$

where $\delta_l = \text{Arg}\ \Gamma(l+1-\frac{iZ}{k})$ is the Coulomb phase shift in the $l^{\text{th}}$ partial wave. We adopt this definition of the phase together with the asymptotic behavior of the radial part of the bare atom continuum wave function that reads:

$$\phi_{E_k}^l(r) \sim \sin(kr + \frac{Z}{k}\ln(2kr) - \frac{l\pi}{2} + \delta_l) \quad \text{for} \quad r \to \infty. \quad (3)$$

The magnetic quantum number $m$ is set to zero due to the linear polarization of the field (which prevents transitions between different $m$'s) and the s-character of the initial state for which $m = 0$.

## 3 Results

### 3.1 ATI spectrum

First of all, we examine the spectrum (Fig. 2) of electrons emitted when shining an ultrashort linearly polarized laser pulse onto atomic cesium. The field is defined as:

$$\mathcal{E}(t) = \mathcal{E}_0 \mathrm{e}^{-(\frac{t}{2\tau})^2} \cos(\omega t + \phi) \quad (4)$$

with the following characteristics: laser wavelength of 620 nm ($\hbar\omega = 2$ eV), a Gaussian pulse ($\tau = 1.75\ T$) with a Full Width at Half Maximum (FWHM) of 6 fs and a peak intensity ($E_0 = 1.19 \times 10^{-3}$ a.u.) of $5 \times 10^{10}$ W/cm$^2$. We have chosen cesium in this study because at this wavelength it ionizes *via* two-photon absorption which requires not too strong fields, reducing thus the complications of strong field effects. The electron spectrum clearly shows the typical features of ATI, namely a succession of peaks with diminishing heights representing the production of electrons with energy:

$$E_k^{(N+S)} = E_{\text{g}} + (N+S)\omega - I_{\text{p}} \quad (5)$$

where $N$ is the net minimum number of photons absorbed to ionize the atom and $S$ the extra photons absorbed in

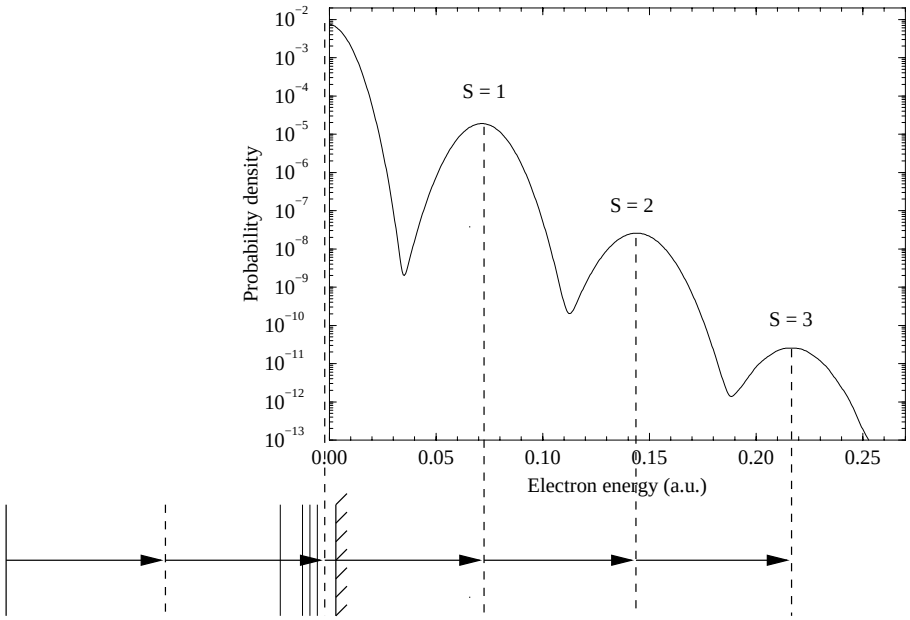


**Fig. 2.** ATI spectrum of cesium shined by a 6 fs pulse with peak intensity of $5\times 10^{10}$ W/cm$^2$ and wavelength of 620 nm ($\phi = 0$).

the continuum. The atom is initially in its ground state of energy $E_{\rm g}$ and its ionization potential is $I_{\rm p}$. The interesting feature appearing in the spectrum and resulting from the pulse shortness, is the rather broad profile of each peak. This broadening is only due to the Fourier limitation of the pulse. As a matter of fact, the peak widths, respectively 0.54 eV, 0.63 eV and 0.70 eV for the peaks $S = 1$, 2 and 3, are comparable with the Fourier bandwidth of the pulse, *i.e.* 0.60 eV. Note that the broadening due to the time-dependent threshold shift is negligible here since the ponderomotive energy doesn't exceed one thousandth of the photon energy; one of the reasons for having chosen Cs. As noted above, all peaks have the same width namely that of the pulse, irrespective of their order. This may seem at variance with the usual picture of resonant few-photon processes under fluctuating field where it is commonly understood that the effective bandwidth in an $N$-photon process is $N\gamma$ where $\gamma$ is the laser bandwidth. Perhaps, the best way to understand the difference is to note that $N$-photon ionization with a Fourier limited pulse is a coherent process from the initial to the final state without any intermediate steps interrupting the coherence. Moreover the field undergoes no stochastic fluctuations [4] whose correlation function leads to an enhancement of the ionization rate and also an apparent effective bandwidth $N\gamma$. In the present case, the process is singly proportional to the $N^{\rm th}$ power of the intensity.

We have calculated the angular distributions of the ATI peaks and found them to be in very good agreement with AD measured in similar conditions [5]. The comparison is shown for the peak $S = 1$ on graph (f) of Figure 3. The present spectrum and ATI peak AD are easily understood and qualitatively predictable with the simple use of lowest order perturbation theory, with the additional fact that spectra are strongly broadened by the Fourier bandwidth due to the shortness of the pulse. For that reason it is more convenient to use a non-perturbative time-dependent calculation which automatically includes the effect of the bandwidth. Our objective here is not to study the properties of the ATI peaks but rather to investigate features at photoelectron energies between the peaks.

### 3.2 Off-energy peak angular distribution

The aim of this section is to focus attention on the electrons emitted in the range of energy located between the peaks $S = 0$ and $S = 1$, in the vicinity of the dip which occurs in the electron spectrum (see Fig. 2). Specifically, we have computed the electron AD for a set of energies ranging from 0.02 a.u. to 0.05 a.u. The main feature to be noted (Fig. 3) is the asymmetric AD of electrons arising in graphs (b) to (e). The first and last graphs correspond to AD at the respective peaks $S = 0$ and $S = 1$. As expected, they show a perfectly symmetric shape (with respect to 90°) as they are measured or simply calculated in perturbation theory for example. Peak $S = 0$ corresponds to the electrons emitted *via* the net absorption of 2 photons while peak $S = 1$ involves 3 photons. Due to the dipole selection rule (the laser is linearly polarized), ATI peak $S = 0$ contains only electrons of even parity (*i.e.* electrons with angular momenta $0, 2, 4, \ldots$) while ATI peak $S = 1$ has an odd parity (angular momenta $1, 3, 5, \ldots$). In either case, each peak is built up as a sum of transitions amplitudes of the same parity thus resulting in symmetric AD, which is in accordance with the usual understanding of photoionization with or without ATI. Although within perturbation theory regime, the maximum angular momentum for the peaks $S = 0$ and $S = 1$ would be respectively 2 and 3, we have indicated above, further angular momenta which may make small contributions beyond lowest order perturbation theory, but do not affect the essential of our arguments as we have checked in the calculation.

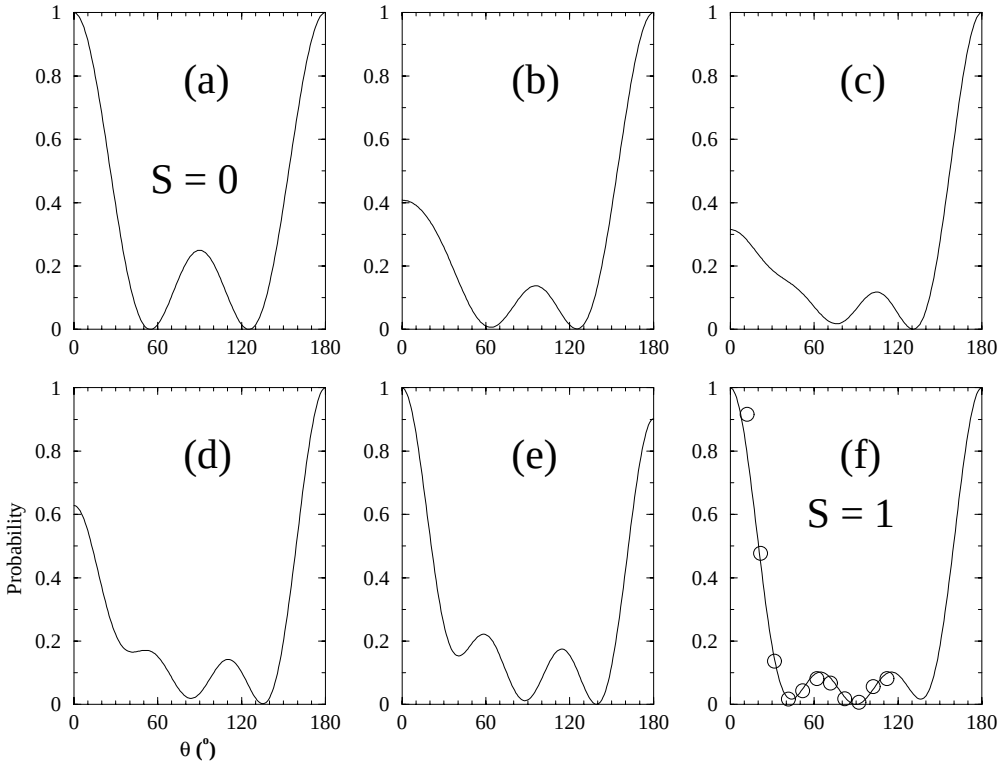


**Fig. 3.** Angular distribution around the first minimum of the ATI spectrum *i.e.* at electron energies: (a) 0 a.u. (S=0), (b) 0.033 a.u., (c) 0.0345 a.u., (d) 0.03525 a.u., (e) 0.036 a.u., (f) 0.0714 a.u. ($S = 1$). Circles refers to experimental data [4] ($\phi = 0$).

However, the situation changes when the electron energy approaches the position of the dip: the AD becomes significantly asymmetric. The shortness of the pulse induces a substantial broadening of the ATI peaks as can be seen in Figure 2. Thus, as we move away from the ATI peak main energy, the probability of observing electrons having the peak parity obviously diminishes but remains significant half a photon-energy away from the peak central energy (midway between the two peaks). The same argument holds for the adjacent peak (of opposite parity) so that the amplitude of electrons emitted with energy lying in between two peaks contains contributions from either peak and therefore parity. We are now in the case where the AD is made of odd and even parity electrons (*i.e.* electrons with angular momentum of $0, 1, 2, 3, 4, \ldots$) which obviously breaks the backward/forward symmetry on to the $x-y$ plane for light linearly polarized along the $z$-axis. The only physical reason for this latter feature is that due to the large Fourier bandwidth, there are energy ranges in the ATI spectrum where electrons have opposite parity with comparable amplitude. Note that the shorter the pulse duration, the stronger the mixing.

### 3.3 Influence of the field initial phase on AD

So far, we have discussed the possible existence of asymmetric AD provided that the field is Fourier limited and that the electrons measured have an energy lying in between two consecutive ATI peaks of the electron spectrum. Figure 4 shows the probability density of emitting an electron in the direction of the laser polarization ($\theta_{\mathbf{k}} = 0°$) as a function of the initial phase of the field $\phi$ (see Eq. (4)). The three curves respectively relate to electron energy of: $E_k = 0.03225$ a.u. (see Fig. 5 energy positions), $E_k = 0.0345$ a.u. and $E_k = 0.03825$ a.u. All curves exhibit significant variations of the probability as the field phase ranges from 0 to $2\pi$ (the total fluctuations are reported also in Fig. 5). In that case, the relative change in the ionization is, respectively, 59%, 75% and 57%. Obviously, this variation vanishes as the electron energy

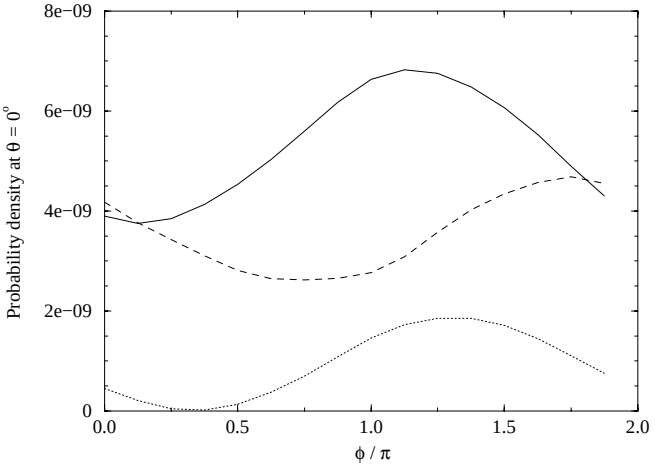


**Fig. 4.** Ionization probability in the direction of the polarization ($\theta_{\mathbf{k}} = 0°$) as a function of the initial phase of the field for electron energies around the dip. The curves correspond to the energies for which the fluctuations are plotted in Figure 5.

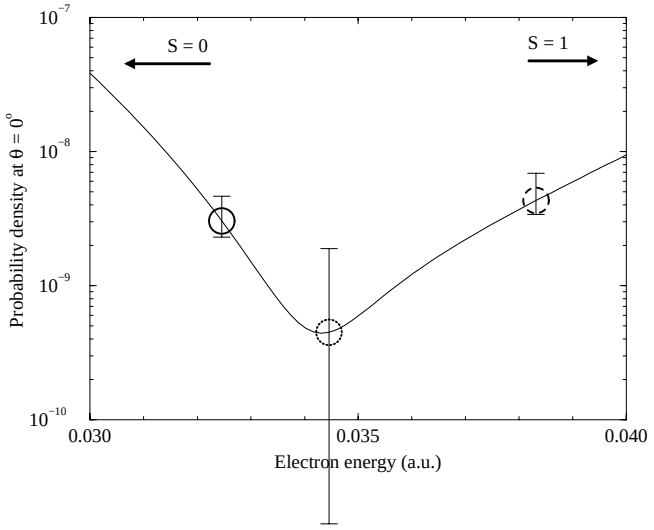


**Fig. 5.** Fluctuations of the probability as a function of the initial phase of the field are reported on the electron spectrum.

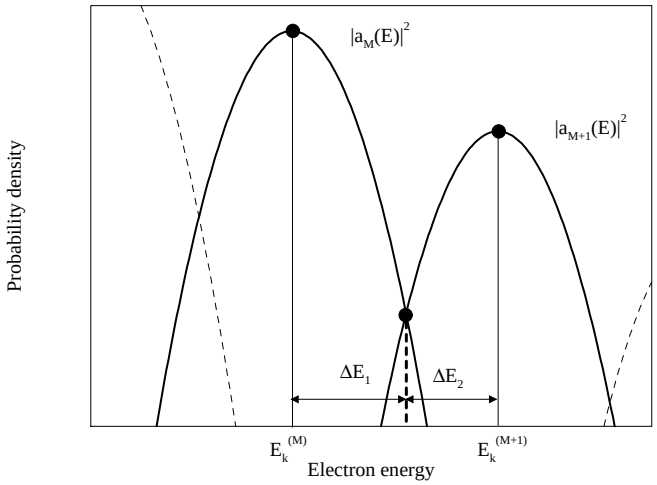


**Fig. 6.** Schematic representation of the electron spectrum near peaks $M$ and $M+1$.

approaches a central peak energy, since for those energies, the AD are perfectly symmetric as explained above. On the other hand, it can be large in the vicinity of the dip. Note that the variations are bigger than 50% on an energy range of at least 0.2 eV around the dip. This interval, which corresponds to a relative value $\frac{\Delta E_k}{E_k}$ close to 20% is compatible with the commonly achieved experimental energy resolution.

The explanation can be made straightforward. The features discussed above are present whenever the energy of the electrons measured is between two consecutive ATI peaks in the electron spectrum, although it was illustrated only by considering the first (2-photon absorption) and the second ((2+1)-photon absorption) peaks. Let $\mathcal{A}_M$ be the total probability amplitude associated with the following process: starting from the ground state, an electron is brought up into the continuum *via* the total net absorption of $M$ photons. This amplitude which includes all possible paths allowed by the dipole selection rule (linear polarization) and eventually higher order processes (more photons involved), lead to the so called ATI peak located in the electron spectrum at an energy defined by equation (5). Since the electromagnetic field amplitude is of the form:

$$\mathcal{E}(t) = \mathcal{E}_o f(t) \mathrm{e}^{i(\omega t+\phi)} \tag{6}$$

and since the process is of order $M$, the amplitude varies like:

$$\mathcal{A}_M = A_M \mathcal{E}_o^M \mathrm{e}^{iM\phi} \tag{7}$$

where $A_M$ is the multiphoton coupling between the ground state and the final continuum state at energy $E_k^{(M)} = E_\mathrm{g} + M\omega - I_\mathrm{p}$. Within perturbation theory, this term is independent of the field. In our case, however, it might be weakly dependent since higher order processes are involved. Nevertheless, we will assume it constant for the sake of simplicity, as we have estimated that our argument is not affected by such a weak intensity dependence.

Since the laser pulse is very short, the field frequency has a broad bandwidth. There is, therefore, a non-zero probability of observing an electron emitted with an energy slightly off the ATI peak. The probability amplitude for that observation can be evaluated as:

$$\begin{aligned}\widetilde{\mathcal{A}}_M(E_k) &= A_M \mathcal{E}_o^M g(E_k) \mathrm{e}^{iM\phi} \\ &= a_M(E_k) \mathrm{e}^{iM\phi}\end{aligned} \tag{8}$$

where $g(E)$ is a shape function accounting for the broadening, that depends on the field bandwidth (more or less given by the Fourier transform of the laser pulse). The complex amplitude $a_M(E_k)$ is centered on $E_k^{(M)}$ as shown in Figure 6 and decreases rapidly at the edges. These latter considerations apply, as well, to the adjacent peak, namely, the probability amplitude for observing an electron slightly off the peak $M+1$ reads:

$$\begin{aligned}\widetilde{\mathcal{A}}_{M+1}(E_k) &= A_{M+1} \mathcal{E}_o^{M+1} g(E_k) \mathrm{e}^{i(M+1)\phi} \\ &= a_{M+1}(E_k) \mathrm{e}^{i(M+1)\phi}.\end{aligned} \tag{9}$$

Finally, the probability of observing the electron with an energy somewhere between the peaks $M$ and $M+1$ (see Fig. 6) is given by:

$$\begin{aligned}&P(E_k = E_k^{(M)} + \Delta E_1) \\ &\quad = |\widetilde{\mathcal{A}}_M(E_k^{(M)} + \Delta E_1) + \widetilde{\mathcal{A}}_{M+1}(E_k^{(M+1)} - \Delta E_2)|^2 \\ &\quad = |a_M(E_k^{(M)} + \Delta E_1) \mathrm{e}^{iM\phi} \\ &\qquad + a_{M+1}(E_k^{(M+1)} - \Delta E_2) \mathrm{e}^{i(M+1)\phi}|^2 \\ &\quad = |a_M|^2 + |a_{M+1}|^2 + 2\mathrm{Re}(a_M a_{M+1}^* \mathrm{e}^{-i\phi})\end{aligned} \tag{10}$$

where $\Delta E_1 + \Delta E_2 = \omega$. The energy dependence has been removed from the last line for the sake of clarity but the terms $a_M$ and $a_{M+1}$ refer to the amplitudes at energy $E_k = E_k^{(M)} + \Delta E_1 = E_k^{(M+1)} - \Delta E_2$. Equation (10) simply produces the interference between the two complex amplitudes as the energy is varied.

As expected, $P(E_k^{(M)}) = |a_M(E_k^{(M)})|^2$ since $a_{M+1}(E_k)$ vanishes as $\Delta E_2$ increases (it equals $\omega$ in that case). Similarly, $P(E_k^{(M+1)}) = |a_{M+1}(E_k^{(M+1)})|^2$. In both cases, the dependence on the phase of the field disappears. On the other hand, the interference grows as $|a_M|$ becomes of the order of $|a_{M+1}|$ to be theoretically of maximum amplitude (with zero minimum) when the two moduli match. This is in complete agreement with the 3 curves plotted in Figure 4 for the case $M = 2$, although the electron energy for which the interference amplitude is maximum is not shown here, the reason being that so far from the ATI peak central energy, the shape function decreases very rapidly and the very position where the two amplitudes intercept (where they have the same modulus) is rather peaked. An experimental attempt to resolve this minimum with high resolution may be difficult, but, as mentioned earlier, the interference modulations are sufficiently important over a range of energy which is compatible with experimental resolution. An important point here is that the interference pattern is rather independent of the ATI peak number. Equation (10) shows that for an arbitrary process of order $M$, the field phase appears as $\mathrm{e}^{-i\phi}$ in the interference term and therefore varies slowly with respect to $\phi$ independently of the process order. Looking at electrons higher in the electron spectrum (higher $M$'s) will lead to the same observation with the difference that the absolute amplitude decreases as the ATI spectrum globally diminishes for high electron energy.

The energy dependent amplitudes $a_M$ and $a_{M+1}$ are complex numbers, so that the term $a_M a_{M+1}^*$ of equation (10) can be written as:

$$a_M a_{M+1}^* = |a_M||a_{M+1}|\mathrm{e}^{i\theta} \tag{11}$$

where both the modulus and the phase depend on the electron energy. Thus, the interference term in equation (10) simply is:

$$2\mathrm{Re}(a_M a_{M+1}^* \mathrm{e}^{-i\phi}) = 2|a_M||a_{M+1}|\cos(\phi - \theta). \tag{12}$$

This latter equation perfectly matches the behavior shown in Figure 4.

Let us summarize at this point the features we have found and their origin. The main effect is the asymmetry (with respect to $\theta_{\mathbf{k}} = 90°$) of photoelectron ADs, when the energy of the detected photoelectron lies off the peak, becoming most pronounced at the minimum. For ultrashort pulses, in the sense defined in the beginning, the peaks are quite broad which makes the signal off the peak non-negligible. Two factors influence this asymmetry: (a) the mixing (coexistence) of even and odd partial waves in the observed photoelectron final state and (b) the sensitivity of the amplitude to the initial phase of the pulse; which means the number of cycles, and in particular fraction thereof during which significant signal is produced. Both produce observable effects for ultrashort pulses, but they do so for different reasons.

To disentangle their influence conceptually, note first that if the value of the initial phase from pulse to pulse varies randomly, a signal integrated over many pulses will show no trace of that dependence. The effect due to the mixing of odd and even partial waves, however will remain. Given that the present aim of ultrashort pulse laser development is to produce pulses of very few cycles with controllable initial phase, it may not be too long before that effect will need to be taken into consideration in photoionization, even when integrated over many pulses. In that case, fluctuations of the initial phase (from pulse to pulse) around some value may also be accounted for in a photoionization signal or even be detected through the analysis of the asymmetry of the AD, depending on the intention of the study. An estimate of the relevant cross-sections for Cs as well as the existence of previous experimental data [5] suggests that even fairly deeply into the minimum these issues are within experimental reach. And it is for this reason that high repetition rate is significant in making up for low signal per pulse.

Part of the work of E.C. was supported by the E.E.C. Human Capital and Mobility program under contract No: CT 930 481. Also part of the work of E.C. was supported by the Laboratoire de Recherche Correspondant du CEA DSM-97-05.

## References

1. E. Cormier, P. Lambropoulos, J. Phys. B **29**, 1667 (1996).
2. E. Cormier, P. Lambropoulos, J. Phys. B **30**, 77 (1997).
3. H. Xu, Ph.D. Thesis, University of southern California, 1993.
4. P. Agostini, A.T. Georges, S.E. Wheatley, P. Lambropoulos, M.D. Levenson, J. Phys. B **11**, 1733 (1978).
5. W. Nicklich, H. Kumpfmüller, H. Walther, X. Tang, H. Xu, P. Lambropoulos, Phys. Rev. Lett. 69, 3455 (1992).